



Research article

Investigation of more solitary waves solutions of the stochastic Benjamin-Bona-Mahony equation under beta operator

Abdelkader Moumen¹, Khaled A. Aldwoah², Muntasir Suhail^{3,*}, Alwaleed Kamel^{2,*}, Hicham Saber¹, Manel Hleili⁴ and Sayed Saifullah⁵

¹ Department of Mathematics, College of Science, University of Ha'il, Ha'il 55473, Saudi Arabia

² Department of Mathematics, Faculty of Science, Islamic University of Madinah, Madinah 42351, Saudi Arabia

³ Department of Mathematics, College of Science, Qassim University, Buraydah 51452, Saudi Arabia

⁴ Department of Mathematics, Faculty of Science, University of Tabuk, P.O. Box 741, Tabuk 71491, Saudi Arabia

⁵ Department of Mathematics and Physics, University of Campania "Luigi Vanvitelli", Caserta 81100, Italy

* **Correspondence:** Email: m.suhail@qu.edu.sa; kalwaleed@iu.edu.sa.

Abstract: This study explores the stochastic Benjamin-Bona-Mahony (BBM) equation with a beta derivative (BD), thereby incorporating multiplicative noise in the Itô sense. We derive various analytical soliton solutions for these equations utilizing two distinct expansion methods: the $\frac{\mathcal{G}'}{\mathcal{G}'+\mathcal{G}+\mathcal{A}}$ -expansion and the modified $\frac{\mathcal{G}'}{\mathcal{G}^2}$ -expansion techniques, both within the framework of beta derivatives. A fractional multistep transformation is employed to convert the equations into nonlinear forms with respect to an independent variable. After performing an algebraic manipulation, the solutions are trigonometric and hyperbolic trigonometric functions. Our analysis demonstrates that the wave behavior is influenced by the fractional-order derivative in the proposed equations, thus providing deeper insights into the wave composition as the fractional order either increases or decreases. Additionally, we explore the effect of white noise on the propagation of the waves solutions. This study underscores the computational robustness and adaptability of the proposed approach to investigate various phenomena in the physical sciences and engineering.

Keywords: Benjamin-Bona-Mahony equation; fractional derivatives; $\frac{\mathcal{G}'}{\mathcal{G}'+\mathcal{G}+\mathcal{A}}$ -expansion method; modified $\frac{\mathcal{G}'}{\mathcal{G}^2}$ -expansion strategy; partial differential equations

Mathematics Subject Classification: 35C05, 35C07, 35C08

1. Introduction

Nonlinear partial differential equations (PDEs) impart multi-scale characteristics to the system, thereby allowing for a more accurate prediction of the transmission process of soliton solutions. In practical uses, nonlinear PDEs and soliton solutions are vital for characterizing various phenomena in science and engineering such as biology, physics, ocean engineering, and many more [1–3]. Various types of soliton solutions have been reported for integrable systems. For instance, horse-shoe like soliton and lump chain solitons have been studied for the elliptic cylindrical Kadomtsev–Petviashvili equation [4]. Yang et al. analyzed degenerating lump chains into anomalously scattered lumps for the Mel’nikov equation [5]. In literature [6], a series of ripple waves with decay modes for the (3+1)-dimensional Kadomtsev–Petviashvili equation have been reported. Rogue wave solutions to the (3+1)-dimensional Korteweg-de Vries Benjamin–Bona–Mahony equation were studied via the Hirota bilinear approach [7]. The propagation features and interactions of Rossby waves soliton of the geophysical equation were studied [8]. Breather, lump, and its interaction solutions for the higher dimensional evolution equation were studied [9]. Multisoliton solutions for the variable coefficient Schrödinger equation has been explored in the literature [10]. Some other solitons solutions have been reported for the regularized long-wave equation [11], the Sharma–Tasso–Olver–Burgers equation [12], the modified Schrödinger’s equation [13], the complex Ginzburg–Landau equation [14], the (2+1) dimensional Chaffee–Infante equation [15], and many more [16–18].

Stochastic differential equations (DEs) deal with phenomena having randomness or uncertainties. Stochastic DEs can be used in various field of science and engineering [19–21]. Solving stochastic nonlinear PDEs is very challenging and hard due to randomness. Therefore, various methods have been introduced and implemented to derive solutions of stochastic PDEs such as the modified tanh method [22], the modified Kudrayshov technique [23], the Sardar subequation method [24], and many more [25, 26].

Fractional operators (FOs) have been frequently used for modelling the physical phenomena in various fields due to its memory process [27–29]. In literature, several FOs have been constructed by researchers and scientists [30–32]. Most of them do not satisfy some properties such as the chain and quotient rules. A few years ago, Atangana [33] defined a local FO called beta derivative, which generalized the classical operator. The beta derivative (BD) is defined as follows:

$$\mathcal{D}_x^\beta \Psi(x) = \frac{d^\beta \Psi}{dx^\beta} = \lim_{h_0 \rightarrow 0} \frac{\Psi\left(x + h_0\left(x + \frac{1}{\Gamma(\beta)}\right)^{1-\beta} - \Psi(x)\right)}{h_0}, \quad 0 < \beta \leq 1.$$

Here, the *BD* has the following characteristics: For every real numbers, m and n :

- (1) $\mathcal{D}_x^\beta \Psi(x) = \left(x + \frac{1}{\Gamma(\beta)}\right)^{1-\beta} \frac{d\Psi}{dx}$.
- (2) $\mathcal{D}_x^\beta (m\Psi + n\Phi) = m\left(x + \frac{1}{\Gamma(\beta)}\right)^{1-\beta} \frac{d\Psi}{dx} + n\left(x + \frac{1}{\Gamma(\beta)}\right)^{1-\beta} \frac{d\Phi}{dx}$.
- (3) $\mathcal{D}_x^\beta (\Psi \circ \Phi(x)) = \left(x + \frac{1}{\Gamma(\beta)}\right)^{1-\beta} \frac{d\Psi}{dx} \Phi'(x) (\Psi'(x))$.
- (4) $\mathcal{D}_x^\beta \Psi(m) = 0$.

The *BD* has been used for the analysis of soliton solutions with the fractional behavior of nonlinear PDEs [34–36]. This work modifies the Benjamin-Bona-Mahony equation (BBME) as follows:

$$\mathcal{M}_t + 6\mathcal{M}\mathcal{D}_x^\beta \mathcal{M} + \mathcal{D}_{xxx}^\beta \mathcal{M} - \rho \mathcal{D}_{xx}^\beta \mathcal{M}_t = \tau \left(\mathcal{M} - \rho \mathcal{D}_{xx}^\beta \mathcal{M} \right) \frac{d\mathcal{P}}{dt}, \quad (1.1)$$

where ρ is real parameter, $\mathcal{M} = \mathcal{M}(x, t)$ is a real valued wave profile, τ is the intensity of sound, and $\mathcal{P} = \mathcal{P}(t)$ is a white noise having the following properties:

(i) \mathcal{P} possesses constant trajectories.

(ii) $\mathcal{P}(0) = 0$.

(iii) $\mathcal{P}(t_{j+1}) - \mathcal{P}(t_j)$ has a normal standard distribution.

When we consider $\tau = 0$ and $\beta = 1$, we get the BBME as follows:

$$\mathcal{M}_t + 6\mathcal{M}\mathcal{M}_x + \mathcal{M}_{xxx} - \rho \mathcal{M}_{xt} = 0. \quad (1.2)$$

Benjamin, Bona, and Mahony examined equation (1.2) as an adjustment to the KdV equation. The BBME has been used to analyze the propagation of long surface gravity pulses with small amplitudes. There are several studies on the BBME. For instance, BBME was studied by using the variational method [37], the deep learning method [38], the generalized exp-function method [39], and many more [40, 41]. In [42], the authors have used the F-expansion method to study the solitary waves BBME under BD with white noise. In this paper, we use two advanced analytical methods to deduce more solitary waves solutions and to study the influence of the BD and the white noise.

2. The general procedure of the proposed approaches

This section provides the general procedure of the suggested approaches that one can use to find solitary and other waves solutions.

2.1. $\frac{\mathcal{G}'}{\mathcal{G}'+\mathcal{G}+\mathcal{A}}$ -expansion method

Here, we present the general procedure of the $\frac{\mathcal{G}'}{\mathcal{G}'+\mathcal{G}+\mathcal{A}}$ -expansion technique. Consider a PDE under space *BD* as follows

$$\mathcal{A}_1 \left(\mathcal{M}, \partial_x^\beta \mathcal{M}, \partial_t \mathcal{M}, \partial_x^\beta \partial_x^\beta \mathcal{M}, \partial_x^\beta \partial_t \mathcal{M}, \partial_t \partial_t \mathcal{M}, \dots \right) = 0, \quad (2.1)$$

where \mathcal{A}_1 is a polynomial in $\mathcal{M} = \mathcal{M}(x, t)$ and its partial derivatives. To use the proposed procedure, one should abide by the following:

Step 1. First using the wave transformation, one can obtain ODE as follows:

$$\mathcal{M}(x, t) = \mathcal{M}(\omega_1) e^{\tau\mathcal{P}(t) - \frac{1}{2}\tau^2 t}, \quad (2.2)$$

where $\omega_1 = \frac{\xi_1}{\beta} \left(x + \frac{1}{\Gamma(\beta)} \right)^\beta + \xi_2 t$. Additionally, ξ_1 and ξ_2 are referred to as the wave speed and the wave number, respectively. By inserting Eq (2.2) in Eq (2.1), the following will be obtained:

$$\mathcal{A}_1 \left(\mathcal{M}, \mathcal{M}', \mathcal{M}'', \mathcal{M}''' \right) = 0, \quad (2.3)$$

where the ordinary derivatives of different orders are indicated by primes.

Step 2. According to the proposed strategy, we examine the following form for the solution to Eq (2.3):

$$\mathcal{M}(\omega_1) = \sum_{i=0}^{\aleph} \mathcal{F}_i \left(\frac{\mathcal{G}'(\omega_1)}{\mathcal{G}'(\omega_1) + \mathcal{G}(\omega_1) + \mathcal{A}} \right)^i, \quad (2.4)$$

where \mathcal{F}_i is the function of the polynomial's coefficients $\left(\frac{\mathcal{G}'}{\mathcal{G}+\mathcal{G}+\mathcal{A}}\right)^i$, $i = 0, 1, 2, \dots, \aleph$. Assume that $\mathcal{G}(\omega_1)$ is a function that fulfills the subsequent relation:

$$\mathcal{G}'' + \mathcal{A}\mathcal{G}' + \mathcal{B}\mathcal{G} + \mathcal{B}\mathcal{A} = 0. \quad (2.5)$$

The value of \aleph can be determined using the homogeneous balance rule (HBR) between the highest nonlinear term and the highest order derivative in Eq (2.3).

Step 3. In this step, the result obtained from the substitution of Eq (2.4) into Eq (2.3) and the coefficients of various powers of $\left(\frac{\mathcal{G}'}{\mathcal{G}+\mathcal{G}+\mathcal{A}}\right)$ should be compared in terms of $\mathcal{A}, \mathcal{B}, \xi_1, \xi_2$, and $i = 0, 1, 2, \dots, \aleph$. Using Mathematica or any other mathematical package, one can determine the solution's values \mathcal{G} in the term $\left(\frac{\mathcal{G}'}{\mathcal{G}+\mathcal{G}+\mathcal{A}}\right)$, and ultimately for the principles of $\left(\frac{\mathcal{G}'}{\mathcal{G}+\mathcal{G}+\mathcal{A}}\right)$, \mathcal{F}_i and ω_1 . In doing so, the solution of Eq (2.2) can be obtained.

2.2. The modified $\frac{\mathcal{G}'}{\mathcal{G}^2}$ -expansion approach

Here, we present the general procedure of applying the modified $\frac{\mathcal{G}'}{\mathcal{G}^2}$ -expansion approach to obtain the wave solutions of a nonlinear PDE. This approach contains the following expansion:

$$\mathcal{M}(\omega_1) = \mathcal{F}_0 + \sum_{i=1}^{\aleph} \left(\mathcal{F}_i \left(\frac{\mathcal{G}'(\omega_1)}{\mathcal{G}(\omega_1)^2} \right)^i + \mathcal{S}_i \left(\frac{\mathcal{G}'(\omega_1)}{\mathcal{G}(\omega_1)^2} \right)^{-i} \right), \quad (2.6)$$

where $\mathcal{G}(\omega_1)$ satisfies the following the equation:

$$\mathcal{G}''(\omega_1) = \frac{\Psi\mathcal{G}'(\omega_1)^2}{\mathcal{G}(\omega_1)^2} + \psi\mathcal{G}'(\omega_1) + \frac{2\mathcal{G}'(\omega_1)^2}{\mathcal{G}(\omega_1)} + \varpi\mathcal{G}(\omega_1)^2, \quad (2.7)$$

where Ψ, ψ , and ϖ are the arbitrary constants. Next, one should find the value of \aleph as previously mentioned. Then, substituting Eq (2.6) and using Eq (2.7) into Eq (2.3), one can obtain a differential equation in $\mathcal{G}(\omega_1)$. Then, collecting those terms which contain $\left(\frac{\mathcal{G}'}{\mathcal{G}^2}\right)^i$, ($i = 0, 1, 2, \dots, n$), and setting all the coefficients of $\left(\frac{\mathcal{G}'}{\mathcal{G}^2}\right)^i$ equal to zero, one can acquire a system of algebraic equations. Solving the obtained system can possibly result in the following families.

Family 1. If $\Psi\varpi > 0$ and $\psi = 0$, the we have the following:

$$\frac{\mathcal{G}'}{\mathcal{G}^2} = \frac{\sqrt{\Psi\varpi} \left(p_1 \cos(\omega_1 \sqrt{\Psi\varpi}) + p_2 \sin(\omega_1 \sqrt{\Psi\varpi}) \right)}{\varpi \left(p_2 \cos(\omega_1 \sqrt{\Psi\varpi}) - p_1 \sin(\omega_1 \sqrt{\Psi\varpi}) \right)}, \quad (2.8)$$

where p_1, p_2, Ψ , and ϖ are arbitrary constants.

Family 2. If $\Psi\varpi < 0$ and $\psi = 0$, then we have the following:

$$\frac{\mathcal{G}'}{\mathcal{G}^2} = -\frac{\sqrt{\Psi\varpi} \left(p_1 \sinh(2\omega_1 \sqrt{\Psi\varpi}) + p_1 \cosh(2\omega_1 \sqrt{\Psi\varpi}) + p_2 \right)}{\varpi \left(p_1 \sinh(2\omega_1 \sqrt{\Psi\varpi}) + p_1 \cosh(2\omega_1 \sqrt{\Psi\varpi}) + p_2 \right)}. \quad (2.9)$$

3. Traveling wave solutions of considered equation

Here, we explore the wave solutions for the proposed stochastic BBME under BD as given in Eq (1.1) with the following procedure:

$$\mathcal{M}(x, t) = \mathcal{M}(\omega_1) e^{\tau \mathcal{P}(t) - \frac{1}{2} \tau^2 t}. \quad (3.1)$$

Furthermore, we have the following:

$$\mathcal{M}_t = \left(\xi_2 \mathcal{M}' + \tau \mathcal{M} \mathcal{P}_t + \frac{1}{2} \tau^2 \mathcal{M} - \frac{1}{2} \tau^2 \mathcal{M} \right) e^{\tau \mathcal{P}(t) - \frac{1}{2} \tau^2 t}, \quad (3.2)$$

and

$$\begin{aligned} \mathcal{D}_{xx}^\beta \mathcal{M}_t &= \left(\xi_1^2 \xi_2 \mathcal{M}''' + \tau \mathcal{P}_t \xi_1^2 \mathcal{M}'' \right) e^{\tau \mathcal{P}(t) - \frac{1}{2} \tau^2 t}, \\ \mathcal{D}_x^\beta \mathcal{M} &= (\xi_1 \mathcal{M}') e^{\tau \mathcal{P}(t) - \frac{1}{2} \tau^2 t}, \quad \mathcal{D}_{xxx}^\beta \mathcal{M} = (\xi_1^3 \mathcal{M}''') e^{\tau \mathcal{P}(t) - \frac{1}{2} \tau^2 t}. \end{aligned} \quad (3.3)$$

Inserting Eq (3.1) into Eq (1.1) and using Eqs (3.2) and (3.3), we obtain the following:

$$\xi_2 \mathcal{M}' + \left(\xi_1^3 - \rho \xi_1^2 \xi_2 \right) \mathcal{M}''' + 6 \xi_1 \mathcal{M} \mathcal{M}' e^{-\frac{1}{2} \tau^2 t} \mathcal{E} e^{\tau \mathcal{P}(t)} = 0. \quad (3.4)$$

By considering $\mathcal{P}(t)$, the Gaussian process, and $\mathcal{E} e^{\tau \mathcal{P}(t)} = e^{\frac{1}{2} \tau^2 t}$, then, Eq (3.4) becomes:

$$\xi_2 \mathcal{M}' + \left(\xi_1^3 - \rho \xi_1^2 \xi_2 \right) \mathcal{M}''' + 6 \xi_1 \mathcal{M} \mathcal{M}' = 0. \quad (3.5)$$

Integrating Eq (3.5) one time while considering the integration constant to be zero, we obtain the following:

$$\zeta \mathcal{M} + \mathcal{M}'' + \eta \mathcal{M}^2 = 0, \quad (3.6)$$

where

$$\zeta = \frac{\xi_2}{\xi_1^3 - \rho \xi_1^2 \xi_2}, \quad \eta = \frac{3}{\xi_1^2 - \rho \xi_1 \xi_2}.$$

In Eq (3.6), by using the homogeneous balance principle, we obtain $\aleph = 2$. Now, we have Eq (2.4) in the following form:

$$\mathcal{M}_1(\omega_1) = \mathcal{F}_0 + \mathcal{F}_1 \left(\frac{\mathcal{G}'}{\mathcal{G}' + \mathcal{G} + \mathcal{A}} \right) + \mathcal{F}_2 \left(\frac{\mathcal{G}'}{\mathcal{G}' + \mathcal{G} + \mathcal{A}} \right)^2. \quad (3.7)$$

Inserting the solution of Eq (3.7) with Eq (2.5) into Eq (3.6), the polynomial of the left side will be in $\left(\frac{\mathcal{G}'}{\mathcal{G}' + \mathcal{G} + \mathcal{A}} \right)^i$, $i = 0, 1, 2 \dots \aleph$. By further equating the coefficients of various powers of $\left(\frac{\mathcal{G}'}{\mathcal{G}' + \mathcal{G} + \mathcal{A}} \right)$ to zero, we obtain a system of algebraic equations. Using Mathematica to solve the system of equations, we obtain the following sets:

$$\begin{cases} \mathcal{F}_0 = \frac{\xi_1 \xi_2 (\mathcal{A}^2 - 12 \mathcal{A} \mathcal{B} + 4 \mathcal{B} (3 \mathcal{B} + 2)) - \xi_2 \sqrt{\xi_1^2 (\mathcal{A}^2 - 4 \mathcal{B})^2}}{6 \xi_1 \sqrt{\xi_1^2 (\mathcal{A}^2 - 4 \mathcal{B})^2}}, \\ \mathcal{F}_1 = \mp \frac{2 \xi_2 (\mathcal{A} - 2 \mathcal{B}) (\mathcal{A} - \mathcal{B} - 1)}{\sqrt{\xi_1^2 (\mathcal{A}^2 - 4 \mathcal{B})^2}}, \quad \mathcal{F}_2 = \frac{2 \xi_2 (-\mathcal{A} + \mathcal{B} + 1)^2}{\sqrt{\xi_1^2 (\mathcal{A}^2 - 4 \mathcal{B})^2}}, \\ \rho = \frac{\frac{\xi_1^2}{\sqrt{\xi_1^2 (\mathcal{A}^2 - 4 \mathcal{B})^2} + \frac{\xi_1^4}{\xi_2}}}{\xi_1^3}. \end{cases} \quad (3.8)$$

Now, inserting the parameter values presented in Eq (3.8) into Eq (3.7), we get the exact solutions of Eq (3.6) in the following two cases:

Set 1. For $\mathcal{D} = \mathcal{A}^2 - 4\mathcal{B} > 0$, we have the following:

$$\begin{aligned} \mathcal{M}(\omega_1) = & \left(\frac{\xi_1 \xi_2 (\mathcal{A}^2 - 12\mathcal{A}\mathcal{B} + (12\mathcal{B}^2 + 8\mathcal{B})) - \xi_2 \sqrt{\xi_1^2 (\mathcal{A}^2 - 4\mathcal{B})^2}}{6\xi_1 \sqrt{\xi_1^2 (\mathcal{A}^2 - 4\mathcal{B})^2}} \right. \\ & - \frac{(2\xi_2(\mathcal{A} - 2\mathcal{B})(\mathcal{A} - \mathcal{B} - 1)) (v_2 e^{\sqrt{\mathcal{D}}\omega_1} (\mathcal{A} - \sqrt{\mathcal{D}}) + v_1 (\sqrt{\mathcal{D}} + \mathcal{A}))}{\sqrt{\xi_1^2 (\mathcal{A}^2 - 4\mathcal{B})^2} (v_2 e^{\sqrt{\mathcal{D}}\omega_1} (-\sqrt{\mathcal{D}} + \mathcal{A} - 2) + v_1 (\sqrt{\mathcal{D}} + \mathcal{A} - 2))} \\ & \left. \frac{(2\xi_2(-\mathcal{A} + \mathcal{B} + 1)^2) \left(\frac{v_2 e^{\sqrt{\mathcal{D}}\omega_1} (\mathcal{A} - \sqrt{\mathcal{D}}) + v_1 (\sqrt{\mathcal{D}} + \mathcal{A})}{v_2 e^{\sqrt{\mathcal{D}}\omega_1} (-\sqrt{\mathcal{D}} + \mathcal{A} - 2) + v_1 (\sqrt{\mathcal{D}} + \mathcal{A} - 2)} \right)^2}{\sqrt{\xi_1^2 (\mathcal{A}^2 - 4\mathcal{B})^2}} \right) e^{\tau\mathcal{P}(t) - \frac{1}{2}\tau^2 t}, \end{aligned} \quad (3.9)$$

where v_1 and v_2 remain constants.

Set 2. For $\mathcal{D} = \mathcal{A}^2 - 4\mathcal{B} < 0$, we have the following:

$$\begin{aligned} \mathcal{M}(\omega_1) = & \left(\frac{\xi_1 \xi_2 (\mathcal{A}^2 - 12\mathcal{A}\mathcal{B} + (12\mathcal{B}^2 + 8\mathcal{B})) - \xi_2 \sqrt{\xi_1^2 (\mathcal{A}^2 - 4\mathcal{B})^2}}{6\xi_1 \sqrt{\xi_1^2 (\mathcal{A}^2 - 4\mathcal{B})^2}} \right. \\ & - \frac{(2\xi_2(\mathcal{A} - 2\mathcal{B})(\mathcal{A} - \mathcal{B} - 1))}{\sqrt{\xi_1^2 (\mathcal{A}^2 - 4\mathcal{B})^2}} \\ & \frac{(\mathcal{A}v_2 + v_1 \sqrt{-\mathcal{D}}) \sin\left(\frac{\sqrt{-\mathcal{D}}}{2}\right) + (\mathcal{A}v_1 - v_2 \sqrt{-\mathcal{D}}) \cos\left(\frac{\sqrt{-\mathcal{D}}}{2}\right)}{((\mathcal{A} - 2)v_2 + v_1 \sqrt{-\mathcal{D}}) \sin\left(\frac{\sqrt{-\mathcal{D}}}{2}\right) + ((\mathcal{A} - 2)v_1 - v_2 \sqrt{-\mathcal{D}}) \cos\left(\frac{\sqrt{-\mathcal{D}}}{2}\right)} \\ & \frac{(2\xi_2(-\mathcal{A} + \mathcal{B} + 1)^2)}{\sqrt{\xi_1^2 (\mathcal{A}^2 - 4\mathcal{B})^2}} \\ & \left. \left(\frac{(\mathcal{A}v_2 + v_1 \sqrt{-\mathcal{D}}) \sin\left(\frac{\sqrt{-\mathcal{D}}}{2}\right) + (\mathcal{A}v_1 - v_2 \sqrt{-\mathcal{D}}) \cos\left(\frac{\sqrt{-\mathcal{D}}}{2}\right)}{((\mathcal{A} - 2)v_2 + v_1 \sqrt{-\mathcal{D}}) \sin\left(\frac{\sqrt{-\mathcal{D}}}{2}\right) + ((\mathcal{A} - 2)v_1 - v_2 \sqrt{-\mathcal{D}}) \cos\left(\frac{\sqrt{-\mathcal{D}}}{2}\right)} \right)^2 \right) e^{\tau\mathcal{P}(t) - \frac{1}{2}\tau^2 t}. \end{aligned} \quad (3.10)$$

4. Application of modified $\frac{\mathcal{G}'}{\mathcal{G}^2}$ -expansion approach

Since the highest-order nonlinear term and the highest-order derivative term are balanced according to the homogenous balance principle in Eq (3.6), we know that the balance number is $\aleph = 2$. Therefore, we have the following:

$$\mathcal{M}(\omega_1) = \mathcal{F}_0 + \mathcal{F}_1 \frac{\mathcal{G}'}{\mathcal{G}^2} + \mathcal{F}_2 \left(\frac{\mathcal{G}'}{\mathcal{G}^2} \right)^2 + \frac{\mathcal{S}_1}{\frac{\mathcal{G}'}{\mathcal{G}^2}} + \frac{\mathcal{S}_2}{\left(\frac{\mathcal{G}'}{\mathcal{G}^2} \right)^2}. \quad (4.1)$$

Inserting Eq (4.1) with aid of Eq (2.7) into Eq (3.6), and following the same procedure as earlier, we obtain the following:

$$\mathcal{F}_1 = -\frac{2\Psi\xi_1^2\psi}{4\rho\Psi\xi_1^2\varpi + \rho\xi_1^2(-\psi^2) + 1}, \mathcal{F}_2 = -\frac{2\Psi^2\xi_1^2}{4\rho\Psi\xi_1^2\varpi + \rho\xi_1^2(-\psi^2) + 1}, \quad (4.2)$$

$$\mathcal{S}_1 = 0, \mathcal{S}_2 = 0, \xi_2 = \frac{\xi_1^3(4\Psi\varpi - \psi^2)}{4\rho\Psi\xi_1^2\varpi + \rho\xi_1^2(-\psi^2) + 1}, \mathcal{F}_0 = -\frac{2\Psi\xi_1^2\varpi}{\rho\xi_1^2(4\varpi\Psi - \psi^2) + 1}.$$

Putting the values of the parameters presented in Eq (4.1) into Eq (3.6) and making use of Eqs (2.8) and (2.9), we obtain the following exact solutions.

Family 1. If $\Psi\varpi > 0$ and $\psi = 0$, then we have the following:

$$\mathcal{M}(\omega_1) = \left(-\frac{(2\Psi^2\xi_1^2) \left(\frac{\sqrt{\Psi\varpi}(p_1\cos(\omega_1\sqrt{\Psi\varpi}) + p_2\sin(\omega_1\sqrt{\Psi\varpi}))}{\varpi(p_2\cos(\omega_1\sqrt{\Psi\varpi}) - p_1\sin(\omega_1\sqrt{\Psi\varpi}))^2} \right)^2}{4\Psi\xi_1^2\varpi\rho + 1} - \frac{2\Psi\xi_1^2\varpi}{4\Psi\xi_1^2\varpi\rho + 1} \right) e^{\tau\mathcal{P}(t) - \frac{1}{2}\tau^2 t}. \quad (4.3)$$

Family 2. If $\Psi\varpi < 0$ and $\psi = 0$, then we have the following:

$$\mathcal{M}(\omega_1) = \left(-\frac{(2\Psi^2\xi_1^2) \left(-\frac{\sqrt{\Psi\varpi}(p_1\sinh(2\omega_1\sqrt{\Psi\varpi}) + p_1\cosh(2\omega_1\sqrt{\Psi\varpi}) + p_2)}{(\varpi(p_1\sinh(2\omega_1\sqrt{\Psi\varpi}) + p_1\cosh(2\omega_1\sqrt{\Psi\varpi}) + p_2))^2} \right)^2}{4\Psi\xi_1^2\varpi\rho + 1} - \frac{2\Psi\xi_1^2\varpi}{4\Psi\xi_1^2\varpi\rho + 1} \right) e^{\tau\mathcal{P}(t) - \frac{1}{2}\tau^2 t}.$$

5. Graphical analysis

This portion of the present work graphically visualize the obtained solutions and presents some physical interpretations and discussions on the obtained results. In Figure 1, solution (3.9) with particular values (i.e, $\nu_1 = 5$, $\nu_2 = -.5$, $\xi_1 = -.2$, $\xi_2 = -1$, $\mathcal{A} = 3$, $\mathcal{B} = 2.6$, $\tau = 0$, $\mathcal{P} = 0$) is visualized. In Figure1, the value of β is varied while the noise intensity τ is considered as zero. The β is used as 1, 0.9, and 0.8 for subfigures (1a,1d), (1b,1e), and (1c,1f), respectively. Here, we observed the dark soliton wave, where we see that as the fractional order decreases when the wave separation is increased.

Furthermore, Figure 2 shows the dynamics of the exact solution (2.2) by varying the noise intensity while keeping the $\beta = 0.95$. Other parameters are used for the simulation of Figure 1. The τ is used as 0.1, 0.4, and 0.9 for subfigures (2a,2d), which is (2b,2e), and (2c,2f), respectively. In Figure 2, one can observe the affects of noise on the dynamics of the solution, which is simulated here. Furthermore, the dynamics of the exact solution (3.10) are visualized in Figures 3 and 4 by varying β and τ , respectively. In the simulation of these figures, the parameters are selected in the form $\nu_1 = .5$, $\nu_2 = 1$, $\xi_1 = -.7$, $\xi_2 = .5$, $p_1 = 2$, $p_2 = 1$, $\mathcal{A} = -4$, $\mathcal{B} = 0$, $\tau = 0$, $\mathcal{P} = 0$; alternatively in Figure 3, the τ is considered as zero. and in Figure 4. the β is fixed as 0.95. The β is used as 1, 0.9, and 0.8 for subfigures (3a,3d), (3b,3e), and (3c,3f), respectively. Similarly, τ is used as 0.2, 0.5, and 0.8 for subfigures (4a,4d), (4b,4e), and (4c,4f), respectively. Here, we observed the interaction of the bright wave with a kink wave, where

the amplitude of the bright wave decreases as the β decreases in the negative region of the spatial coordinate.

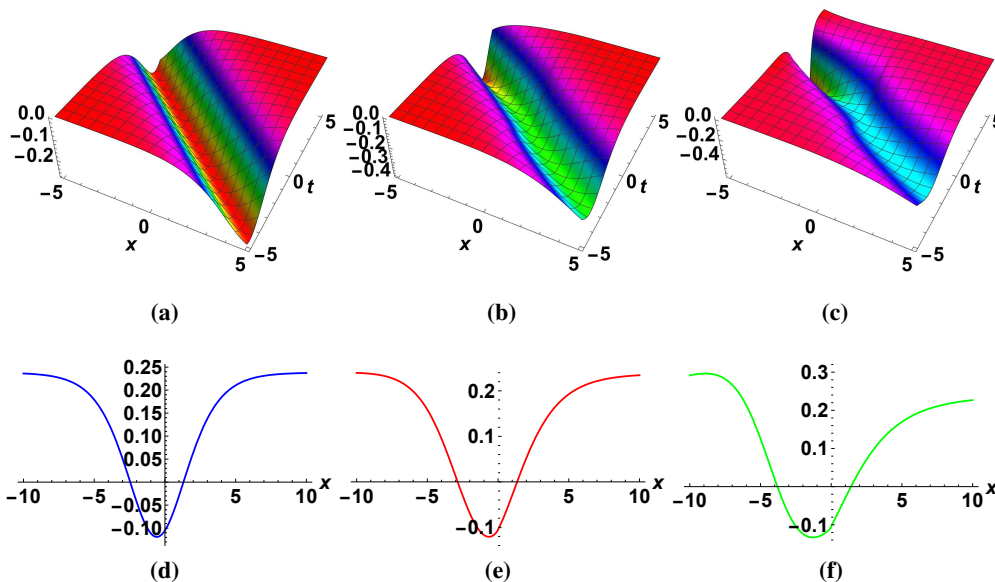


Figure 1. The visualization of exact solution (2.2) with $v_1 = .5, v_2 = 1, \xi_1 = -.7, \xi_2 = .5, p_1 = 2, p_2 = 1, \mathcal{A} = -3, \mathcal{B} = 0, \tau = 0, \mathcal{P} = 0, \tau = 0$ and varying β .

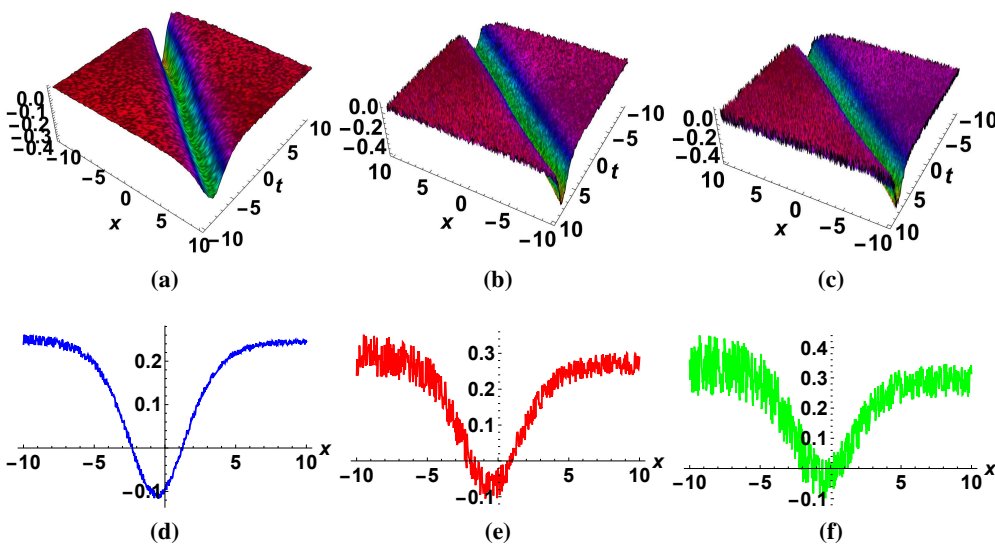


Figure 2. The visualization of exact solution (2.2) with $v_1 = .5, v_2 = 1, \xi_1 = -.7, \xi_2 = .5, p_1 = 2, p_2 = 1, \mathcal{A} = -3, \mathcal{B} = 0, \mathcal{P} = 0.5, \beta = 0.95.$ and varying τ .

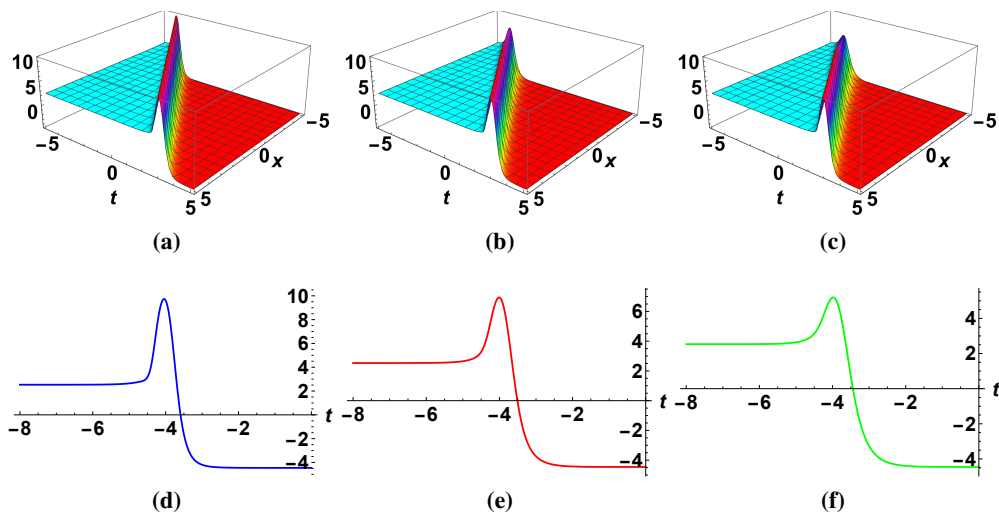


Figure 3. The visualization of solution $v_1 = .5, v_2 = 1, \xi_1 = -.7, \xi_2 = .5, p_1 = 2, p_2 = 1, \mathcal{A} = -4, \mathcal{B} = 0, \mathcal{P} = 0, \tau = 0$ and different values of β .

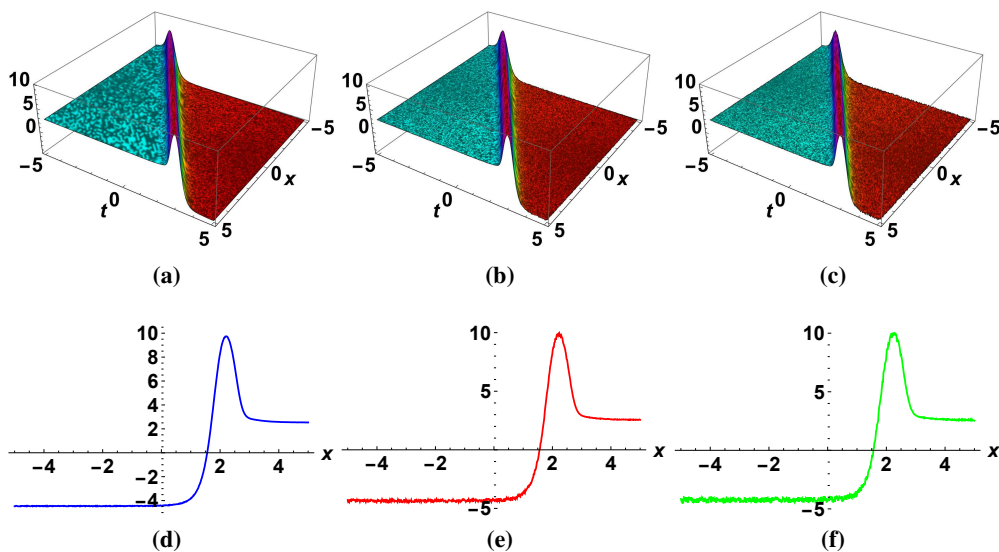


Figure 4. The visualization of solution $v_1 = .5, v_2 = 1, \xi_1 = -.7, \xi_2 = .5, p_1 = 2, p_2 = 1, \mathcal{A} = -4, \mathcal{B} = 0, \mathcal{P} = 0, \beta = 0.95$ and different values of τ .

In Figure 5, the solution (3.9) with particular values (i.e, $v_1 = 5, v_2 = -.5, \xi_1 = -.2, \xi_2 = -1, \mathcal{A} = 3, \mathcal{B} = 2.6, \tau = 0,$ and $\mathcal{P} = 0$) is visualized. In Figure 5, the various values for β are considered, while the noise intensity τ is supposed to be zero. The β is considered as 1, 0.95, and 0.9 for subfigures (5a,5d), (5b,5e), and (5c,5f), respectively. Here, we observed the hybrid bright-dark soliton wave, where we see that as the fractional order decreases when then amplitude of the dark solitons increases and the bright soliton is decreases.

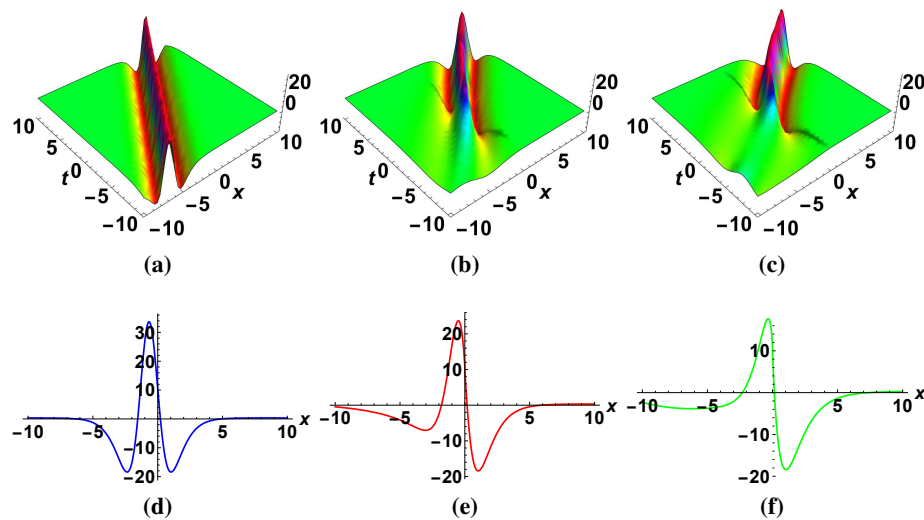


Figure 5. The visualization of solution with $\rho = 1, \varpi = -.1, \xi_1 = 1, \Psi = 1, p_1 = 1, p_2 = 1, \mathcal{P} = 0, \tau = 0$, and varying β .

Moreover, Figure 6 shows the dynamics of the exact solution (3.9) by varying the noise intensity while keeping the $\beta = 0.95$. Other parameters are used for the simulation of Figure 5. The τ is used as 0.5, 0.6, and 0.9 for subfigures (6a,6d), (6b,6e), and (6c,6f), respectively. In Figure 6, one can observe the affects of noise on the dynamics of the solution, which is simulated here; it can be seen that the highest and lowest amplitude areas become more random as τ increases.

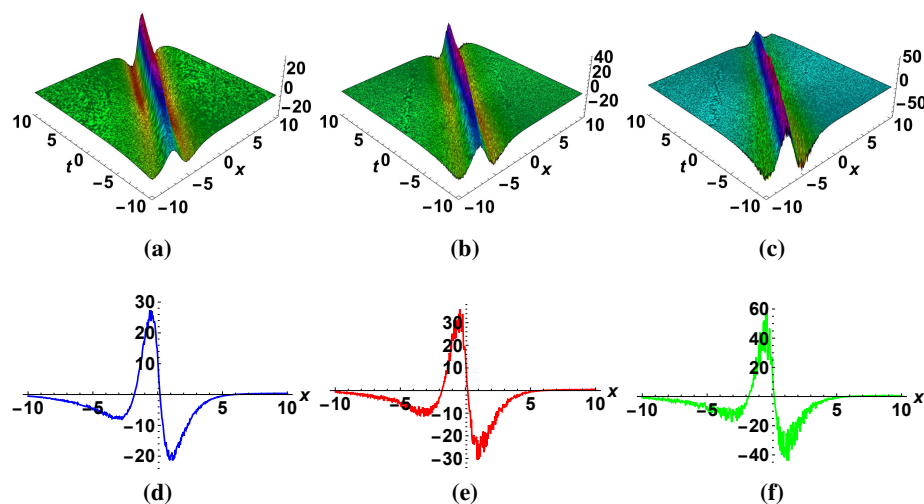


Figure 6. The visualization of solution with $\rho = 1, \varpi = -.1, \xi_1 = 1, \Psi = 1, p_1 = 1, p_2 = 1, \mathcal{P} = 0, \beta = 0.95$ and varying τ .

Furthermore, the dynamics of the exact solution (3.10) are visualized in Figures 7 and 8 by varying β and τ , respectively. In the simulation of these figures, the parameters are selected in the form $\rho = 1, \varpi = -.1, \xi_1 = 1, \Psi = 1, p_1 = 1, p_2 = 1, \mathcal{P} = 0$, and $\tau = 0$; alternatively, in Figure 7, the τ is considered as zero, and in Figure 8, the β is fixed as 0.95. The β is used as 1, 0.9, and 0.8 for

subfigures (7a,7d), (7b,7e), and (7c,7f), respectively. Similarly, τ is used as 0.05, 0.3, and 0.6 for subfigures (8a,8d), (8b,8e), and (8c,4f), respectively. Here, we observed the periodic wave solution, where the amplitude of the periodic waves decreases as the β decreases in the negative region of the spatial coordinate. Furthermore, we see that the wave profile behaves more randomly in areas where the amplitude is either low or high. Thus, from these analyses, it can be noticed that the obtained results are more generalized than the solutions reported in previous papers. Indeed, when the BD operators equals one, the solution converges to the stochastic integer order solutions. If the intensity of the white noise is zero, then the solutions converge to a deterministic case. When $\beta = 1$ and $\tau = 0$, the obtained solutions converge to the deterministic case.

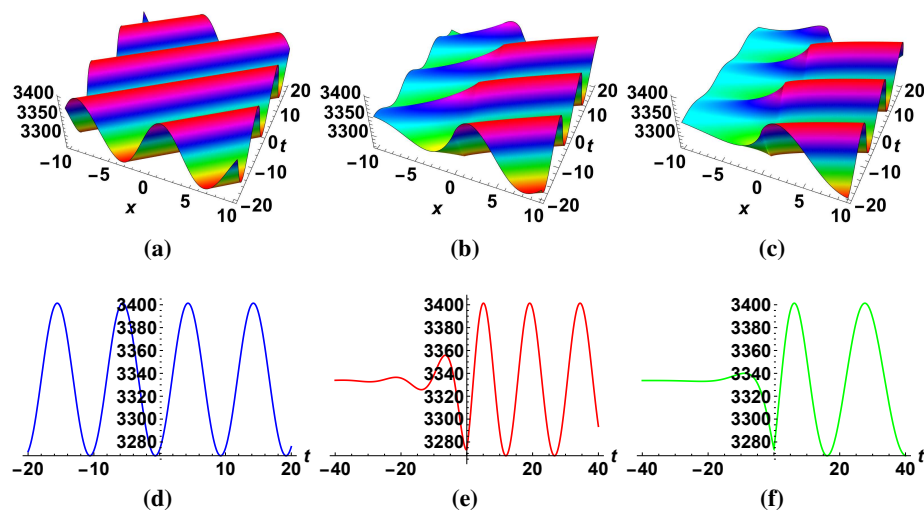


Figure 7. The visualization of solution with $\rho = 1, \varpi = -1, \xi_1 = 1, \Psi = 1, p_1 = 1, p_2 = 1, \mathcal{P} = 0, \tau = 0$ and varying β .

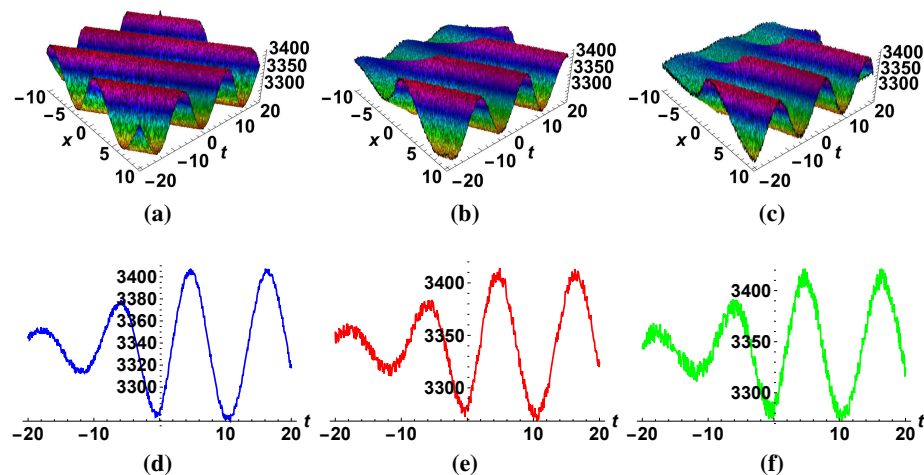


Figure 8. The visualization of solution with $\rho = 1, \varpi = -1, \xi_1 = 1, \Psi = 1, p_1 = 1, p_2 = 1, \mathcal{P} = 0, \beta = 0.95$ and varying τ .

6. Conclusions

This study has explored the stochastic BBME with the BD, thereby incorporating multiplicative noise in the Itô sense. We have derived various analytical soliton solutions for these equations by utilizing two distinct expansion methods, both within the framework of beta derivatives. A fractional multistep transformation was employed to convert the equations into nonlinear forms with respect to an independent variable. After performing algebraic manipulations, the solutions were found to be trigonometric and hyperbolic trigonometric functions. Our analysis demonstrated that the wave behavior was influenced by the fractional-order derivative in the proposed equations, thus providing deeper insights into the wave composition as the fractional order increases or decreases. Additionally, we examined the effect of white noise on the propagation of wave solutions. This study has underscored the computational robustness and adaptability of the proposed approach to investigate various phenomena in the physical sciences and engineering.

Author contributions

Conceptualization: M.S.D.S. Methodology: K.A.A. Software: S.S. Validation: A.K. Formal analysis: A.K. Investigation: M.H. Writing-original draft preparation: K.A.A. Writing-review and editing: H.S., A.M.

Acknowledgments

The Researchers would like to thank the Deanship of Graduate Studies and Scientific Research at Qassim University for financial support (QU-APC-2024-9/1). The authors wish to extend their sincere gratitude to the Deanship of Scientific Research at the Islamic University of Madinah.

Conflict of interest

All authors declare no conflicts of interest in this paper.

References

1. M. Bilal, U. Younas, J. Ren, Dynamics of exact soliton solutions in the double-chain model of deoxyribonucleic acid, *Math. Method. Appl. Sci.*, **44** (2021), 13357–13375. <https://doi.org/10.1002/mma.7631>
2. S. Javeed, K. S. Alimgeer, S. Nawaz, A. Waheed, M. Suleman, D. Baleanu, et al., Soliton solutions of mathematical physics models using the exponential function technique, *Symmetry*, **12** (2020), 176. <https://doi.org/10.3390/sym12010176>
3. İ. Yalçınkaya, H. Ahmad, O. Tasbozan, A. Kurt, Soliton solutions for time fractional ocean engineering models with Beta derivative, *J. Ocean Eng. Sci.*, **7** (2022), 444–448. <https://doi.org/10.1016/j.joes.2021.09.015>

4. X. Yang, Z. Wang, Z. Zhang, Solitons and lump waves to the elliptic cylindrical Kadomtsev–Petviashvili equation, *Commun. Nonlinear Sci.*, **131** (2024), 107837. <https://doi.org/10.1016/j.cnsns.2024.107837>
5. X. Yang, Z. Wang, Z. Zhang, Generation of anomalously scattered lumps via lump chains degeneration within the Mel’nikov equation, *Nonlinear Dyn.*, **111** (2023), 15293–15307. <https://doi.org/10.1007/s11071-023-08615-3>
6. X. Yang, Z. Wang, Z. Zhang, Decay mode ripple waves within the (3+1)-dimensional Kadomtsev–Petviashvili equation, *Math. Method. Appl. Sci.*, **47** (2024), 10444–10461. <https://doi.org/10.1002/mma.10132>
7. X. Yang, Z. Zhang, A. Wazwaz, Z. Wang, A direct method for generating rogue wave solutions to the (3+1)-dimensional Korteweg-de Vries Benjamin-Bona-Mahony equation, *Phys. Lett. A*, **449** (2022), 128355. <https://doi.org/10.1016/j.physleta.2022.128355>
8. X. Yin, L. Xu, L. Yang, Evolution and interaction of soliton solutions of Rossby waves in geophysical fluid mechanics, *Nonlinear Dyn.*, **111** (2023), 12433–12445. <https://doi.org/10.1007/s11071-023-08424-8>
9. N. Cao, X. Yin, S. Bai, L. Xu, Breather wave, lump type and interaction solutions for a high dimensional evolution model, *Chaos Soliton. Fract.*, **172** (2023), 113505. <https://doi.org/10.1016/j.chaos.2023.113505>
10. L. Xu, X. Yin, N. Cao, S. Bai, Multi-soliton solutions of a variable coefficient Schrödinger equation derived from vorticity equation, *Nonlinear Dyn.*, **112** (2024), 2197–2208. <https://doi.org/10.1007/s11071-023-09158-3>
11. Y. Kai, J. Ji, Z. Yin, Study of the generalization of regularized long-wave equation, *Nonlinear Dyn.*, **107** (2022), 2745–2752. <https://doi.org/10.1007/s11071-021-07115-6>
12. Y. Kai, Z. Yin, Linear structure and soliton molecules of Sharma-Tasso-Olver-Burgers equation, *Phys. Lett. A*, **452** (2022), 128430. <https://doi.org/10.1016/j.physleta.2022.128430>
13. C. Zhu, M. Al-Dossari, S. Rezapour, S. Shateyi, On the exact soliton solutions and different wave structures to the modified Schrödinger’s equation, *Results Phys.*, **54** (2023), 107037. <https://doi.org/10.1016/j.rinp.2023.107037>
14. C. Zhu, M. Al-Dossari, S. Rezapour, S. A. M. Alsallami, B. Gunay, Bifurcations, chaotic behavior, and optical solutions for the complex Ginzburg–Landau equation, *Results Phys.*, **59** (2024), 107601. <https://doi.org/10.1016/j.rinp.2024.107601>
15. C. Zhu, M. Al-Dossari, S. Rezapour, B. Gunay, On the exact soliton solutions and different wave structures to the (2+1) dimensional Chaffee–Infante equation, *Results Phys.*, **57** (2024), 107431. <https://doi.org/10.1016/j.rinp.2024.107431>
16. C. Zhu, M. Al-Dossari, S. Rezapour, S. Shateyi, B. Gunay, Analytical optical solutions to the nonlinear Zakharov system via logarithmic transformation, *Results Phys.*, **56** (2024), 107298. <https://doi.org/10.1016/j.rinp.2023.107298>
17. S. Ahmad, A. Ullah, S. Ahmad, S. Saifullah, A. Shokri, Periodic solitons of Davey Stewartson Kadomtsev Petviashvili equation in (4+1)-dimension, *Results Phys.*, **50** (2023), 106547. <https://doi.org/10.1016/j.rinp.2023.106547>

18. S. Khaliq, S. Ahmad, A. Ullah, H. Ahmad, S. Saifullah, T. A. Nofal, New waves solutions of the (2+1)-dimensional generalized Hirota–Satsuma–Ito equation using a novel expansion method, *Results Phys.*, **50** (2023), 106450. <https://doi.org/10.1016/j.rinp.2023.106450>
19. M. Z. Baber, N. Ahmed, C. Xu, M. S. Iqbal, T. A. Sulaiman, A computational scheme and its comparison with optical soliton solutions for the stochastic Chen–Lee–Liu equation with sensitivity analysis, *Mod. Phys. Lett. B*, 2024, 2450376. <https://doi.org/10.1142/S0217984924503767>
20. C. Xu, Y. Pang, Z. Liu, J. Shen, M. Liao, P. Li, Insights into COVID-19 stochastic modelling with effects of various transmission rates: Simulations with real statistical data from UK, Australia, Spain, and India, *Phys. Scr.*, **99** (2024), 025218. <https://doi.org/10.1088/1402-4896/ad186c>
21. R. P. King, Applications of stochastic differential equations to chemical-engineering problems-an introductory review, *Chem. Eng. Commun.*, **1** (1974), 221–237. <https://doi.org/10.1080/00986447408960433>
22. I. Samir, H. M. Ahmed, Retrieval of solitons and other wave solutions for stochastic nonlinear Schrödinger equation with non-local nonlinearity using the improved modified extended tanh-function method, *J. Opt.*, 2024. <https://doi.org/10.1007/s12596-024-01776-3>
23. S. Ahmad, S. F. Aldosary, M. A. Khan, Stochastic solitons of a short-wave intermediate dispersive variable (SI_dV) equation, *AIMS Mathematics*, **9** (2024), 10717–10733. <https://doi.org/10.3934/math.2024523>
24. H. Ur Rehman, A. U. Awan, S. M. Eldin, I. Iqbal, Study of optical stochastic solitons of Biswas–Arshed equation with multiplicative noise, *AIMS Mathematics*, **8** (2023), 21606–21621. <https://doi.org/10.3934/math.20231101>
25. A. Secer, Stochastic optical solitons with multiplicative white noise via Itô calculus, *Optik*, **268** (2022), 169831. <https://doi.org/10.1016/j.ijleo.2022.169831>
26. H. Ur Rehman, I. Iqbal, H. Zulfiqar, D. Gholami, H. Rezazadeh, Stochastic soliton solutions of conformable nonlinear stochastic systems processed with multiplicative noise, *Phys. Lett. A*, **486** (2023), 129100. <https://doi.org/10.1016/j.physleta.2023.129100>
27. C. Xu, Y. Zhao, J. Lin, Y. Pang, Z. Liu, J. Shen, et al., Bifurcation investigation and control scheme of fractional neural networks owning multiple delays, *Comp. Appl. Math.*, **43** (2024), 186. <https://doi.org/10.1007/s40314-024-02718-2>
28. C. Xu, M. Farman, A. Shehzad, Analysis and chaotic behavior of a fish farming model with singular and non-singular kernel, *Int. J. Biomath.*, 2023, 2350105. <https://doi.org/10.1142/S179352452350105X>
29. C. Xu, M. Farman, Z. Liu, Y. Pang, Numerical approximation and analysis of epidemic model with constant proportional Caputo operator, *Fractals*, **32** (2024), 2440014. <https://doi.org/10.1142/S0218348X24400140>
30. D. Baleanu, K. Diethelm, E. Scalas, J. J. Trujillo, *Fractional calculus: Models and numerical methods*, World Scientific, 2012. <https://doi.org/10.1142/8180>
31. M. Caputo, M. Fabrizio, A new definition of fractional derivative without singular kernel, *Progr. Fract. Differ. Appl.*, **1** (2015), 73–85.

32. A. Atangana, D. Baleanu, New fractional derivatives with nonlocal and non-singular kernel: Theory and application to heat transfer model, 2016, arXiv: 1602.03408. <https://doi.org/10.48550/arXiv.1602.03408>
33. A. Atangana, D. Baleanu, A. Alsaedi, Analysis of time-fractional Hunter-Saxton equation: A model of neumatic liquid crystal, *Open Phys.*, **14** (2016), 145–149. <https://doi.org/10.1515/phys-2016-0010>
34. A. Yusuf, M. Inc, A. I. Aliyu, D. Baleanu, Optical solitons possessing beta derivative of the Chen-Lee-Liu equation in optical fibers, *Front. Phys.*, **7** (2019), 34. <https://doi.org/10.3389/fphy.2019.00034>
35. Y. Gurefe, The generalized Kudryashov method for the nonlinear fractional partial differential equations with the beta-derivative, *Rev. Mex. Fís.*, **66** (2020), 771–781. <https://doi.org/10.31349/RevMexFis.66.771>
36. H. Ahmad, M. N. Alam, M. A. Rahim, M. F. Alotaibi, M. Omri, The unified technique for the nonlinear time-fractional model with the beta-derivative, *Results Phys.*, **29** (2021), 104785. <https://doi.org/10.1016/j.rinp.2021.104785>
37. K. J. Wang, Variational principle and diverse wave structures of the modified Benjamin-Bona-Mahony equation arising in the optical illusions field, *Axioms*, **11** (2022), 445. <https://doi.org/10.3390/axioms11090445>
38. Q. Liu, Y. Zhou, K. Li, S. Zhang, Application of the dynamical system method and the deep learning method to solve the new (3+1)-dimensional fractional modified Benjamin–Bona–Mahony equation, *Nonlinear Dyn.*, **110** (2022), 3737–3750. <https://doi.org/10.1007/s11071-022-07803-x>
39. M. Shakeel, Attaullah, E. R. El-Zahar, N. A. Shah, J. D. Chung, Generalized exp-function method to find closed form solutions of nonlinear dispersive modified Benjamin–Bona–Mahony equation defined by seismic sea waves, *Mathematics*, **10** (2022), 1026. <https://doi.org/10.3390/math10071026>
40. A. Elmandouh, E. Fadhal, Bifurcation of Exact Solutions for the Space-Fractional Stochastic Modified Benjamin–Bona–Mahony Equation, *Fractal Fract.*, **6** (2022), 718. <https://doi.org/10.3390/fractalfract6120718>
41. Sirendaoreji, Novel solitary and periodic wave solutions of the Benjamin–Bona–Mahony equation via the Weierstrass elliptic function method, *Int. J. Appl. Comput. Math.*, **8** (2022), 223. <https://doi.org/10.1007/s40819-022-01441-y>
42. F. M. Al-Askar, C. Cesarano, W. W. Mohammed, The influence of white noise and the beta derivative on the solutions of the BBM equation, *Axioms*, **12** (2023), 447. <https://doi.org/10.3390/axioms12050447>



AIMS Press

©2024 the Author(s), licensee AIMS Press. This is an open access article distributed under the terms of the Creative Commons Attribution License (<http://creativecommons.org/licenses/by/4.0>)